

LibIQ: Toward Real-Time Spectrum Classification in O-RAN dApps

Filippo Olimpieri*, Noemi Giustini*, Andrea Lacava*†, Salvatore D’Oro†, Tommaso Melodia†, Francesca Cuomo*

*Sapienza University of Rome, Rome, Italy

†Institute for the Wireless Internet of Things, Northeastern University, Boston, MA, USA

Email: {olimpieri.1933529, giustini.1933541}@studenti.uniroma1.it,

Email: {lacava.a, s.doro, t.melodia}@northeastern.edu, {francesca.cuomo}@uniroma1.it

Abstract—The O-RAN architecture is transforming cellular networks by adopting Radio Access Network (RAN) softwarization and disaggregation concepts to enable data-driven monitoring and control of the network. Such management is enabled by RAN Intelligent Controllers (RICs), which facilitate near-real-time and non-real-time network control through xApps and rApps. However, they face limitations, including latency overhead in data exchange between the RAN and RIC, restricting real-time monitoring, and the inability to access user plain data due to privacy and security constraints, hindering use cases like beamforming and spectrum classification. To address these limitations, several architectural proposals have been made, including dApps, i.e., applications deployed within the RAN unit that enable real-time inference, control and Radio Frequency (RF) spectrum analysis. In this paper, we leverage the dApps concept to enable real-time RF spectrum classification with LibIQ, a novel library for RF signals that facilitates efficient spectrum monitoring and signal classification by providing functionalities to read I/Q samples as time-series, create datasets and visualize time-series data through plots and spectrograms. Thanks to LibIQ, I/Q samples can be efficiently processed to detect external RF signals, which are subsequently classified using a Convolutional Neural Network (CNN) inside the library. To achieve accurate spectrum analysis, we created an extensive dataset of time-series-based I/Q samples, representing distinct signal types captured using a custom dApp running on a 5th generation (5G) deployment over the Colosseum network emulator and an Over-The-Air (OTA) testbed. We evaluate our model by deploying LibIQ in heterogeneous scenarios with varying center frequencies, time windows, and external RF signals. In real-time analysis, the model classifies the processed I/Q samples, achieving an average accuracy of approximately 97.8% in identifying signal types across all scenarios.

Index Terms—Open RAN, dApps, Real-Time Control Loops, Spectrum Classification

Filippo Olimpieri and Noemi Giustini contributed equally to this work. This article is based upon work partially supported by OUSD(R&E) through Army Research Laboratory Cooperative Agreement Number W911NF-24-2-0065. The views and conclusions contained in this document are those of the authors and should not be interpreted as representing the official policies, either expressed or implied, of the Army Research Laboratory or the U.S. Government. The U.S. Government is authorized to reproduce and distribute reprints for Government purposes notwithstanding any copyright notation herein. The work was also partially supported by SERICS (PE00000014) 5GSec project, CUP B53C22003990006, under the MUR National Recovery and Resilience Plan funded by the European Union - NextGenerationEU, and by the U.S. National Science Foundation under CNS-1925601.

I. INTRODUCTION

The Open Radio Access Network (RAN) paradigm is gaining momentum in the cellular networks thanks to its open and modular approach that promotes interoperability and innovation by disaggregating the RAN functionalities over white-box hardware and different software components [1]. In the O-RAN architecture, network control is realized through closed control loops—continuous cycles of data collection and control actions, in which specialized applications can adapt the network to evolving conditions. However, in the current standard defined by the O-RAN ALLIANCE, two key limitations persist: the lack of attention for the user-plane and physical-layer data such as I/Q samples, and the support for sub-10 ms control loops, ruling out the real-time feedback needed for advanced low-latency use cases, such as beamforming, spectrum sharing, and more [2]. The introduction of real-time control loops will enable direct action at the lower layers of the RAN, allowing adaptive responses to radio conditions while minimizing delays. Moreover, a direct access to I/Q samples enables classification systems to detect anomalous signals and interference, enhancing attack detection, dynamic resource management, and spectrum sharing to protect network integrity of the 5th generation (5G) and beyond cellular networks. To address these challenges, dApps [3] are introduced as software components deployed alongside Central Unit (CU) and Distributed Unit (DU), where user-plane and I/Q data is directly accessible, enabling Artificial Intelligence (AI)/Machine Learning (ML) routines to operate in real-time within the RAN. However, the challenges of processing large I/Q data in real-time remains, requiring specialized AI/ML models optimized for edge inference [3].

In this paper, we introduce LibIQ¹, a novel library designed to enhance the analysis, manipulation, and labeling of time-series-based I/Q samples, thereby enabling spectrum monitoring and signal classification within dApps. The library supports both frequency-domain and time-domain analysis, offering functionalities such as plots and spectrogram generation, Fast Fourier Transform (FFT) and Power Spectral Density (PSD) calculation. We embed our library in a dApp to

¹LibIQ is publicly available at <https://github.com/wineslab/lib-iq>.

perform spectrum sensing by accessing I/Q samples retrieved from unscheduled Orthogonal Frequency Division Multiplexing (OFDM) symbols to classify in real-time the presence of external Radio Frequency (RF) signals and transmission technologies operating in the same spectral space of the RAN where the dApp is deployed. Such classification is achieved by LibIQ thanks to an internal Convolutional Neural Network (CNN) that is able to detect Radio Frequency Interferences (RFIs) by analyzing time series based I/Q samples in the frequency domain. Such I/Q samples were collected in an extensive data collection campaign with more than 35,200 time series across six different signal types and four center frequencies, varying the time window to analyze temporal patterns. Furthermore, we extend the Graphical User Interface (GUI) currently available in the dApp framework by incorporating the output of our model, i.e., the classification labels assigned to the I/Q samples processed in real-time.

To validate the effectiveness of our approach, we conduct experiments in two different Software-defined Radio (SDR)-based environments: the Colosseum network emulator [4], and an Over-The-Air (OTA) testbed. The main contributions of this work are:

- *LibIQ*, a software library for the parsing, manipulation, visualization, and classification of time series-based I/Q samples;
- The implementation of a high-performance CNN time-series classifier, achieving an average classification accuracy of approximately 97.8% across diverse RF conditions, varying center frequencies, and different time windows;
- The first integration of a spectrum classification process into the dApp framework, allowing experiments while respecting the real-time constraints.

The remainder of this paper is organized as follows: Section II reviews existing literature on the O-RAN architecture and RF spectrum classification; Section III presents the functionalities of LibIQ and its integration in the dApp framework; Section IV details the experimental pipeline that leverages LibIQ; Section V discusses the results of training and testing of the CNN, and Section VI summarizes key findings and outlines future research directions.

II. RELATED WORKS

This section briefly introduces the O-RAN architecture, the concept of dApps and reviews the various approaches proposed in the literature for spectrum classification.

A. O-RAN and dApps

The O-RAN paradigm is a new architectural concept for cellular networks based on disaggregation and programmability of the RAN functions for enabling a multi-vendor, data-driven approach [1]. O-RAN disaggregates the classic Next Generation Node Base (gNB) into CU, DU, and Radio Unit (RU), introducing the RAN Intelligent Controllers (RICs) as the entity responsible for the control and managements of the units through open interfaces. Thanks to this approach, the

RICs become centralized abstractions of the networks that can manage near-real-time and non-real-time tasks through xApps and rApps. However, at the current time, there is no standardized way to access real-time, i.e., sub-10 ms timescales, parameters in the RAN, therefore no real-time control is available. To address these issues, a recent research report [2] from the O-RAN next Generation Research Group (nGRG) explores the concept of dApps. dApps are microservices co-located with CU and DU that enable the real-time exposure and processing of RAN data that otherwise would not be available to the RICs due to latency or privacy constraints [3]. In this paper, we leverage dApps by embedding our library's CNN to classify RF signal types based on processed user-plane data. To the best of our knowledge, this is the first work to apply the dApp framework to perform real-time spectrum classification within the O-RAN context.

B. Spectrum Classification with Deep Learning

Recent research in spectrum sensing and signal classification has explored a range of deep learning techniques to enhance accuracy, efficiency, and adaptability across diverse conditions. Several works have leveraged CNNs to process spectral data, each with distinct methodologies and results.

For instance, [5] applies a residual CNN to normalized power spectrum data for binary spectrum sensing, effectively distinguishing between signal-plus-noise and noise-only scenarios. Meanwhile, [6] integrates a CNN with an Long Short Term Memory (LSTM) to analyze STFT-based spectrograms, achieving high accuracy in identifying wireless technologies such as Wi-Fi and 5G. Other works focus on CNN-based architectures specifically optimized for hardware efficiency. The authors in [7] employ a three-layer CNN designed to minimize computational complexity, making it suitable for embedded systems with constrained processing power. In contrast, [8] transforms I/Q samples into image representations and applies the YOLOv8x object detection model, achieving 77.78% accuracy on a small dataset. Similarly, [9] finds that frequency-domain I/Q samples provide better inputs for CNN-based modulation classification compared to time-domain representations, underscoring the importance of input feature selection.

To improve latency and efficiency, alternative CNN architectures avoid spectrogram conversion. Spectrum Stitching [10] uses a U-Net with a non-local block for direct I/Q processing, reducing computational overhead and speeding up inference. While this method eliminates feature extraction, it requires extensive training to generalize across signal variations, balancing accuracy and efficiency. In the context of O-RAN-based implementations, ChARM [11] provides a real-time, data-driven framework for dynamic spectrum sharing in O-RAN networks, enabling spectrum sensing, interference detection. However, its integration with O-RAN remains unclear, and its classifier handles a limited set of RF signals.

Our approach differs from previous works in multiple aspects. Unlike spectrogram-based classification ([6], [8]) or hardware-efficient CNNs ([7]), we process frequency-domain

I/Q samples directly using a CNN trained on time-series data that performs multinomial classification, in contrast with the binary one of [5]. Before classification, we apply an Energy Peak Detector to isolate relevant signals and reduce dimensionality, optimizing both performance and efficiency. In terms of results, our method achieves 97.8% classification accuracy, significantly outperforming image-based classification ([8], 77.78%) and offering superior real-time adaptability compared to methods based on static spectrograms ([9], approx 90%). Furthermore, our spectrum classification model is the only one that has been tested within a real dApp framework, interacting directly with an operating gNB, unlike previous works that primarily rely on offline datasets or simulated environments or substantial modification of the O-RAN architecture [11].

III. SYSTEM OVERVIEW

This section provides an overview of LibIQ and its integration into a dApp to enable real-time spectrum analysis. LibIQ is implemented in C++ and wrapped in Python using Simplified Wrapper and Interface Generator (SWIG) and has four main components. The order in which the library's packages and classes are presented in this chapter reflects the typical workflow a user can follow to analyze and classify its data.

A. Analyzer: Time series analysis and manipulation

LibIQ provides a package called `Analyzer` that includes a suite of methods enabling users to manipulate and analyze I/Q sample time series. Starting from binary data, LibIQ can parse, extract and select the real or the imaginary component, or both, of the I/Q samples through a set of software functions. Moreover, LibIQ exposes utility functions such as the FFT and PSD to analyze I/Q samples in the frequency domain.

B. Plotter: Time series visualization

The `Plotter` package provides methods for visualize I/Q data. The `scatterplot()` function allows users to generate scatterplots, which are essential for analyze the distribution and characteristics of signal data. These plots can represent the I/Q samples single components or their magnitude and phase. Additionally, it supports spectrogram generation through `spectrogram()` function. This is achieved by dividing the time series into multiple equal parts (windows) and applying the FFT to each of them. Users can customize window size and overlap to adjust the level of detail in the spectrogram. Smaller windows with more overlap capture subtle signal variations, otherwise larger windows with less overlap offer a broader view, highlighting the signal's long-term behavior.

C. Preprocessor: Time Series Preprocessing

The `Preprocessor` package handles data preprocessing phase, ensuring the dataset is correctly formatted and optimized for training. Such parsing is implemented through two key functions: `create_dataset_from_bin()`, which creates a dataset from a binary file, and

`create_dataset_from_csv()`, which processes a CSV file containing time-series-based I/Q samples. Finally, the `energy_peak_detector()` function acts as an Energy Peak Detector that is able to extract and isolate the RFI signal and to ensure that the CNN model is independent from the RFI source center frequency.

D. Classifier: Time Series Classification

The `Classifier` class is responsible for training and testing a CNN model designed for RF signal classification. The training process, managed by `cnn_train()`, involves feeding the model with time series made of I/Q samples, leveraging features such as the real and imaginary parts, magnitude, and phase. The length of each time series, i.e., the time window, can change through different trained models as shown more in details in Section IV. Once trained, the CNN model can be used for classification via the `cnn_test()` function, which takes a pre-trained model and predicts the appropriate label for the input time series.

E. Integration of LibIQ on dApp

As described in Section II, the O-RAN ALLIANCE has introduced xApps and rApps to enable near-real-time and non-real-time closed control loops in the RAN, leaving a gap for the real-time domain. dApps can perform real-time analysis and interference detection without requiring any RIC, thus reducing latency. In this work, we extend the spectrum analysis capabilities of the dApps using LibIQ to create time-series data from the dApp measurements. As shown in Fig. 1, the dApp embeds LibIQ in its real-time control loop to feed the LibIQ pipeline with the I/Q samples. Then LibIQ applies the Energy Peak Detector, calculates the features and classifies such peaks with the CNN. Once the model has assigned a label to the time series, the result is returned to the dApp, which can propagate it to the RIC or, as we did in this work, display it on the dApp GUI beside the "Predicted Label" field in the waterfall plot illustrated in Fig. 1. This dApp-based processing approach offers significant advantages by enabling execution directly at the DU/CU without relying on the RIC. It enhances efficiency by processing user-plane data locally, eliminating the need for high-bandwidth data transfers over external interfaces. The integration of LibIQ enhances network reliability and spectrum analysis by combining real-time processing with AI-driven classification.

IV. REAL-TIME SPECTRUM CLASSIFICATION

In this section, we introduce the experimental pipeline used to accurately classify I/Q data. Our pipeline is designed to efficiently manage every stage of the process, including analysis, visualization, and classification of RFI signals.

A. Dataset collection and preprocessing

We leverage and extend the dApp framework of [3] to access and collect the I/Q samples in real-time. The dApp is designed with a sensing periodicity of approximately 8 ms, meaning it periodically provides data to LibIQ for labeling.

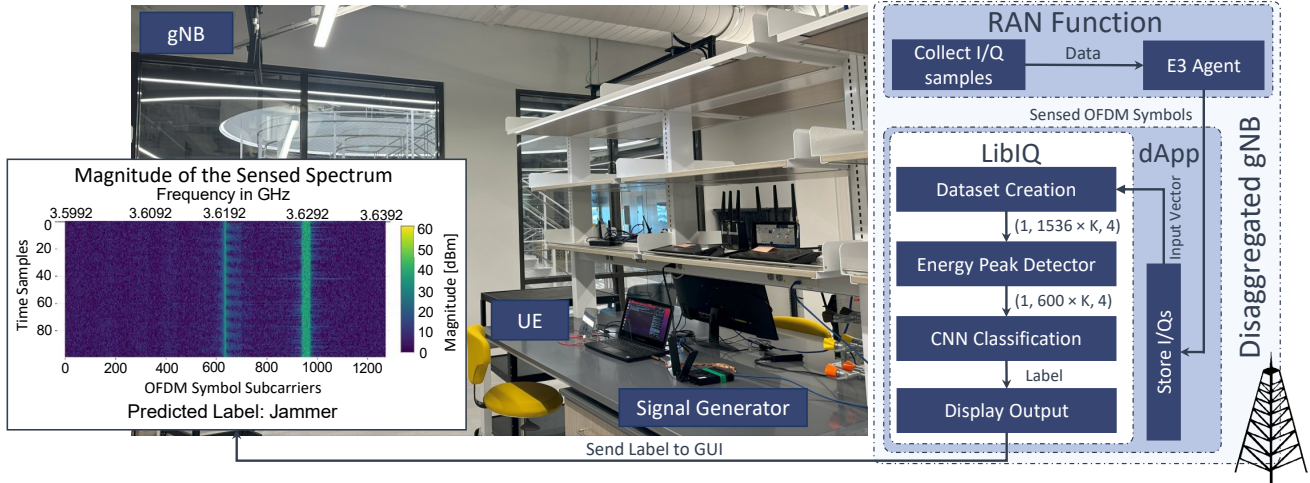


Fig. 1: LibIQ deployment inside an O-RAN dApps.

Once collected, the I/Q samples are organized into complex input vectors, each containing real and imaginary components. Each vector consists of 1,536 I/Q samples, representing data collected from spectrum sensing. These vectors are stored in a binary file, with each file containing 100 input vectors.

We collected data from two different environments: one in an emulated environment using Colosseum [4], and the other in a real environment using transmissions over the air. We use a 5G standalone (SA) deployment of one gNB with OpenAir-Interface (OAI), operating at a center frequency of 3.6192 GHz with a 40 MHz bandwidth that onboard our dApp. As shown in Fig. 1, for the OTA testbed we connect a Commercial Off-the-Shelf (COTS) One Plus Nord phone to the network to generate downlink traffic even though in this work we focus more on the external than the User Equipment (UE) performance. To generate external signals, we employed GNU Radio, the `siggen` utility of the `uhd` library for SDRs, and the SCOPE framework [12], each transmitting different signal types, as shown in Table I. The center frequency of the transmitted signals varied among 3.6042 GHz, 3.6142 GHz, 3.6242 GHz, and 3.6342 GHz, while the sampling rate remained fixed at 1 MHz throughout all transmissions.

We organize the data into a structured format with the shape $(N, 1536 \times K, 4)$, where N represents the total number of time series, while K is the number of I/Q samples within each time series, which varies depending on the time window. In this work, we have tested using time windows of different lengths, i.e., 1, 5, 10, or 15 data samples, to determine how many input vectors are considered for a single prediction. However, such lengths are not fixed and can be changed and adapted within LibIQ. A larger time window provides a broader temporal perspective of the signal, capturing more variations over time. Lastly, the third dimension 4 refers to the number of different features analyzed, i.e., the real part (Q), imaginary part (I), the magnitude, and the phase of the data. We collected about 800 time series for each RFI signal type (LTE, Jammer, No RFI, Square, Triangular, and Radar), each environment, and

each center frequency (four in total), except for LTE, which was registered only in the Colosseum environment, collecting a total of about 35,200 time series. The details of these RFI signals are provided in Table I and illustrated in Fig. 2.

Waveform	Gain [dB]		Amplitude	Label	Software
	OTA	Colosseum			
Sine	90	25	1	1	Radar
Triangular	100	25	1	1	Triangular
Square	100	25	1	1	Square
Uniform	80	20	1	1	Jammer
LTE	/	20	/	0.9	LTE

TABLE I: Waveform types and their assigned labels in the experimental dataset.

Finally, we apply an Energy Peak Detector that identifies the maximum energy peak within a user-defined sliding window. Then, a specified number of samples are extracted from both sides, ensuring that the most relevant portion of the signal is preserved.

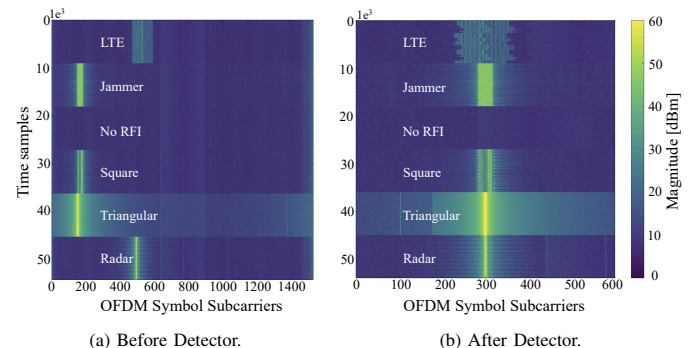


Fig. 2: Comparison of RF data before and after the Energy Peak Detector.

After applying the Energy Peak Detector, the data are reshaped into $(N, J \times K, 4)$, where J is the length of the detector window, set to 600 I/Q samples in our experiments. Figure 2a shows the raw input before detection, where the full

1536-sample sequence contains noise and irrelevant data. In contrast, Figure 2b shows how the detector isolates a shorter segment of samples, centered on the energy peak, that captures the most relevant portion of each RF signal. This reduction in input size decreases computational cost by avoiding analysis of the full spectrum. More importantly, by focusing only on the informative part, it improves the accuracy and generalization of the CNN models while reducing the risk of overfitting.

The dataset collected was used to train and evaluate the performance of the CNN, which will be further discussed in Section V. Specifically, we used two center frequencies for training, while the remaining frequencies were reserved for testing to assess the model’s generalization capability.

B. Data-Driven Spectrum Classification

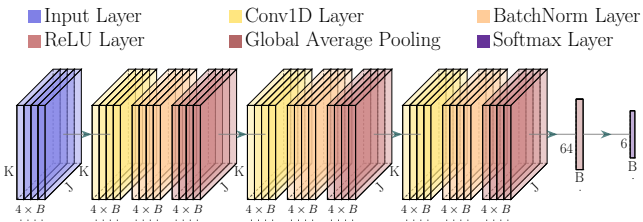


Fig. 3: CNN Architecture for signal classification.

The CNN in our library, represented in Fig. 3, is designed to label time-series of I/Q samples based on the transmission technologies of the signals. The model processes time-series-based I/Q samples with an input shape of $(32, J \times K, 4)$, i.e., the batch size, the total number of I/Q samples $J \times K$ and and the number of distinct features. J denotes the length of each input vector after applying the energy detector and K refers to the number of I/Q samples within each time series, that depends on the time window.

The model begins with an input layer that receives the time-series data. Then, the first convolutional layer applies 64 one-dimensional filters along the time axis with padding, producing an output of dimension equal to $(32, J \times K, 64)$. This is followed by batch normalization that normalizes activations between channels and a ReLU activation function that improves the model’s ability to capture non-linear patterns.

This pattern is repeated three times to allow the CNN to progressively learn more complex features. After this feature extraction process, a global average pooling layer condenses the learned information into a fixed-length feature vector with shape $(32, 64)$. After this phase, the extracted features are passed through a fully connected layer, transforming them into a representation with shape $(32, 6)$ that captures higher-level abstractions of the time-series data. Finally, the model’s output layer is made of a Softmax activation layer, which maps the 6-dimensional representation to a number of output units equal to the number of classes, where each output unit represents the probability of a specific class.

During the training phase, which lasts 10 epochs, the model learns to differentiate between signal types by extracting

relevant features from the dataset previously discussed in Section IV-A. An epoch consists of a complete pass through all the samples in the training set of dimension $(N, J \times K, 4)$ where N is equal to 17600. The choice of N comes from the dataset’s size that contains 35200 time series, with half of the center frequencies allocated for training, and the remaining two are reserved for testing to evaluate the model’s generalization ability. The CNN processes the data in batches of 32 samples so, the number of updates performed during a single epoch is $17600/32 = 550$. This means that the model updates its weights 550 times per epoch through backpropagation. Over the course of 10 epochs, the total number of updates amounts to $550 \times 10 = 5500$.

V. RESULTS

In this section, we evaluate the results of the CNN model and the experiments introduced in this work, summarized in Table II.

Metric	Description	Time Windows [# input vectors]			
		1	5	10	15
Accuracy	Ratio of correct predictions to total predictions	0.979	0.987	0.971	0.976
Precision	Ratio of true positives to all predicted positives	0.982	0.988	0.975	0.979
Recall	Ratio of true positives to all actual positives	0.980	0.987	0.971	0.976
F1 Score	Harmonic mean of precision and recall	0.980	0.972	0.971	0.976
Latency [ms]	Time required for a single prediction	2.23 ±0.48	1.13 ±0.04	0.92 ±0.11	0.90 ±0.05

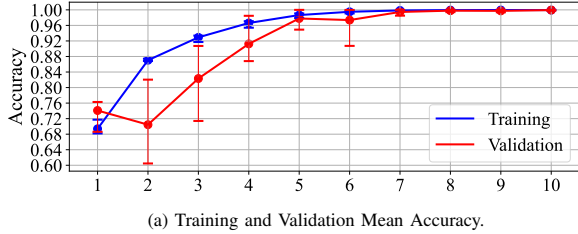
TABLE II: Performance metrics over different time windows.

We use multiple performance indicators to provide a comprehensive evaluation of the model’s effectiveness. Accuracy measures overall correctness, peaking at 98.7% and never dropping below 97.1%. Precision ranges from 97.5% to 98.8% ensuring the model makes correct predictions, and minimizes false positives. Instead, Recall confirms its ability to detect true positives (mean 97.6%). Furthermore, the F1 score remains above 97.1%, confirming a well-balanced trade-off between capturing positive instances and preventing misclassifications.

To evaluate model latency, we ran six three-minute experiments per time window size, computing mean latency and z-scores. As shown in Table II, there is a trade-off between window size and total latency. Larger windows reduce the number of predictions but increase per-prediction time, while smaller windows lead to more frequent, faster predictions, raising overall latency. For example, with equal experiment duration, a window size of 15 produces a single prediction with minimal buffering but higher inference time, whereas a size of 1 yields 15 quicker predictions, increasing cumulative latency. However, latency remains consistently below the 10 ms real-time threshold.

Figures 4a and 4b illustrate the average training and validation accuracy and loss per epoch, respectively, across multiple

experiments. In Figure 4a, the accuracy of training and validation increases rapidly and converges to nearly 100%, indicating fast and effective learning. Similarly, Figure 4b shows a rapid reduction in both training and validation losses, with the two curves remaining closely aligned throughout the process. This alignment suggests a stable training phase and confirms the absence of overfitting.



(a) Training and Validation Mean Accuracy.

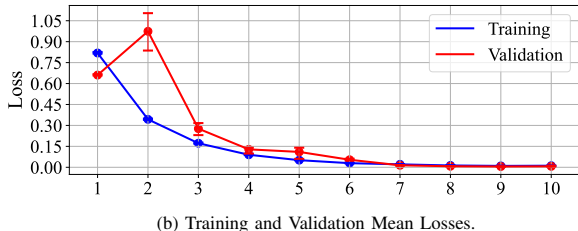


Fig. 4: Training and validation losses and accuracies over epochs.

Lastly, Figure 5 reveals a near-perfect classification accuracy with minimal misclassifications, further demonstrating the robustness and effectiveness of the proposed approach.

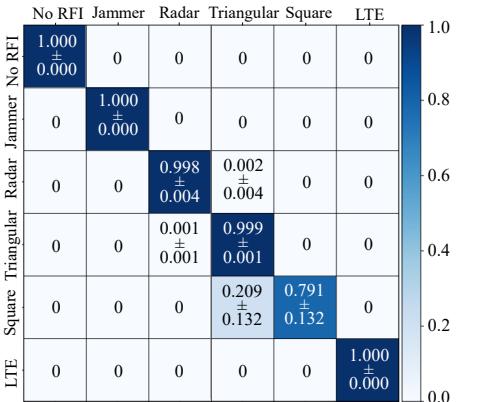


Fig. 5: Predicted vs Real Labels for Signal Classification with Z-score.

VI. CONCLUSIONS AND FUTURE WORK

In this work, we introduce LibIQ, a comprehensive library designed to analyze, manipulate and label time-series-based I/Q samples with high performance. Thanks to its integration with dApps, LibIQ provides a new way to enable real-time analysis methodologies, increasing awareness and paving the way to full control of the spectrum in the O-RAN architecture.

An innovative feature of LibIQ is its CNN classifier, trained on an extensive and diverse dataset of signals to ensure robust and accurate classification. To rigorously evaluate its

performance, we conducted numerous tests in two SDR-based environments, proving the reliability of LibIQ thanks to the combination of the Energy Peak Detector and the CNN classifier. The results demonstrate LibIQ's robustness, as it achieves an average classification accuracy of approximately 97.8% across different scenarios, center frequencies, signal conditions and environments.

Looking ahead, we plan to enhance the dataset by incorporating a broader range of signal types, emerging technologies, and complex network scenarios to improve system robustness. Additionally, we aim to integrate anomaly detection algorithms to enable a deeper analysis of spectral, temporal, and behavioral patterns in I/Q traffic. Finally, a key future direction is to establish a direct connection between the analysis module and the RIC, enabling automated corrective actions and fostering a more intelligent and adaptive RAN environment.

REFERENCES

- [1] M. Polese, L. Bonati, S. D’Oro, S. Basagni, and T. Melodia, “Understanding O-RAN: Architecture, Interfaces, Algorithms, Security, and Research Challenges,” *IEEE Communications Surveys & Tutorials*, 2023.
- [2] Northeastern University, NVIDIA, Mavenir, MITRE, and Qualcomm, “dApps for Real-Time RAN Control: Use Cases and Requirement,” O-RAN next Generation Research Group (nGRG), Research Report, 10 2024, report ID: RR-2024-10. [Online]. Available: <https://mediastorage.o-ran.org/ngrg-rr/nGRG-RR-2024-10-dApp\%20use\%20cases\%20and\%20requirements.pdf>
- [3] A. Lacava, L. Bonati, N. Mohamadi, R. Gangula, F. Kaltenberger, P. Johari, S. D’Oro, F. Cuomo, M. Polese, and T. Melodia, “dApps: Enabling Real-Time AI-Based Open RAN Control,” *arXiv preprint arXiv:2501.16502*, 2025. [Online]. Available: <https://arxiv.org/abs/2501.16502>
- [4] M. Polese, L. Bonati, S. D’Oro, P. Johari, D. Villa, S. Velumani, R. Gangula, M. Tsampazi, C. Paul Robinson, G. Gemmi, A. Lacava, S. Maxenti, H. Cheng, and T. Melodia, “Colosseum: The Open RAN Digital Twin,” *IEEE Open Journal of the Communications Society*, vol. 5, pp. 5452–5466, 2024.
- [5] S. Zheng, S. Chen, P. Qi, H. Zhou, and X. Yang, “Spectrum Sensing Based on Deep Learning Classification for Cognitive Radios,” *China Communications*, vol. 17, no. 2, pp. 138–148, 2020.
- [6] W. Zhang, M. Feng, M. Krantz, and A. H. Y. Abyaneh, “Signal Detection and Classification in Shared Spectrum: A deep Learning Approach,” in *IEEE INFOCOM 2021-IEEE Conference on Computer Communications*. IEEE, 2021, pp. 1–10.
- [7] W. M. Lees, A. Wunderlich, P. J. Jeavons, P. D. Hale, and M. R. Souryal, “Deep Learning Classification of 3.5-GHz Band Spectrograms With Applications To Spectrum Sensing,” *IEEE transactions on cognitive communications and networking*, vol. 5, no. 2, pp. 224–236, 2019.
- [8] A. Amici, L. M. Monteforte, L. Chiaraviglio, and P. Loreti, “RadioDL: Deep Learning-Based Signal Intelligence of IQ Captures,” in *IEEE Wireless Communications and Networking Conference (WCNC)*. IEEE, 2025, pp. 1–6.
- [9] S. C. Hauser, W. C. Headley, and A. J. Michaels, “Signal Detection Effects on Deep Neural Networks Utilizing Raw IQ for Modulation Classification,” in *MILCOM 2017-2017 IEEE Military Communications Conference (MILCOM)*. IEEE, 2017, pp. 121–127.
- [10] D. Uvaydov, M. Zhang, C. P. Robinson, S. D’Oro, T. Melodia, and F. Restuccia, “Stitching the Spectrum: Semantic Spectrum Segmentation with Wideband Signal Stitching,” in *IEEE INFOCOM 2024 - IEEE Conference on Computer Communications*, 2024, pp. 2219–2228.
- [11] L. Baldesi, F. Restuccia, and T. Melodia, “ChARM: NextG Spectrum Sharing Through Data-Driven Real-Time O-RAN Dynamic Control,” in *IEEE INFOCOM 2022 - IEEE Conference on Computer Communications*, 2022, pp. 240–249.
- [12] L. Bonati, S. D’Oro, S. Basagni, and T. Melodia, “SCOPE: An open and Softwarized Prototyping Platform For NextG Systems,” in *Proceedings of the 19th Annual International Conference on Mobile Systems, Applications, and Services*, 2021, pp. 415–426.